JOC Article

Rigid Duplex α-Cyclodextrin Reversibly Connected With Disulfide Bonds. Synthesis and Inclusion Complexes

Lukáš Kumprecht,[†] Miloš Buděšínský,[†] Jiří Vondrášek,[†] Jiří Vymětal,[†] Jiří Černý,[†] Ivana Císařová,[‡] Jiří Brynda,[†] Vladimír Herzig,[†] Petr Koutník,[†] Jiří Závada,[†] and Tomáš Kraus*[,‡]

Institute of Organic Chemistry and Biochemistry AS CR, v.v.i. Flemingovo nám. 2, 166 10 Praha 6, Czech Republic, and Department of Inorganic Chemistry, Charles University, Hlavova 2030, 128 40 Praha 2, Czech Republic

kraus@uochb.cas.cz

Received September 24, 2008

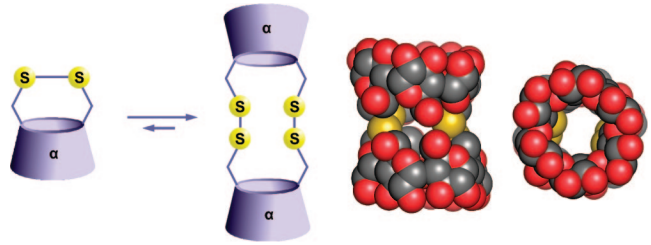

The rigid duplex cyclodextrin **6** composed of two α-cyclodextrin macrocycles connected with two disulfide bonds in "transannular" ($C6^{I}$, $C6^{IV}$) positions was prepared from partially debenzylated α-cyclodextrin **1** in four steps in 73% overall yield. In the last key step involving oxidative coupling of the thiol **5**, predominance of the target duplex **6** can be attained under conditions of thermodynamic control. The structure of duplex cyclodextrin was established by MS as well as 2-D NMR methods and confirmed by a single-crystal X-ray analysis. The ability of the duplex cyclodextrin **6** to bind α,ω-alkanediols (C_9−C_{14}) and 1-alkanols (C_9 and C_{10}) was studied by isothermal titration calorimetry in aqueous solutions. The stability constants of the complexes gradually increase with the alkyl chain length and reach an unprecedently high value of $K = 8.6 \times 10^9$ M^{-1} for 1,14-tetradecanediol. It was found that the doubly bridged dimer **6** exhibits higher binding affinity toward the series of α,ω-alkanediols than the singly bridged analogue **10** by about 2 orders of magnitude in K (M^{-1}) or 3.1−3.3 kcal/mol in $\Delta G°$, the enhancement being due to enthalpic factors. Theoretical calculations using DFT-D methods suggest that the enthalpic contribution stems from dispersion interactions.

Introduction

Cyclodextrins are known to form inclusion complexes with a broad range of organic molecules in aqueous media.[1−4] Owing to this unique property, they have found widespread use in various branches of industry, pharmaceutical in particular. Yet the relatively low stability of the complexes—the average binding constant[4] in water amounts to $10^{2.5\pm1.1}$ M^{-1}—puts severe limits on further development of their applications, particularly in the field of targeted drug delivery (e.g., at micromolar concentration, a complex exhibiting $K = 10^3$ M^{-1} would be

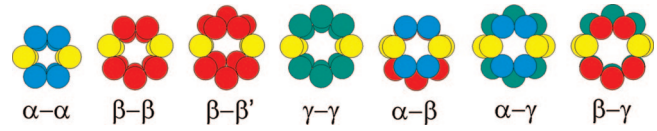

FIGURE 1. Schematic representation of a virtual dynamic library of dimeric species (top-down view) resulting from oxidation reaction of α-, β-, and γ-cyclodextrin derivatives bearing two sulfanil groups in "transanular" $C6^{I}$ and $C6^{IV}$ ($C6^{V}$ of γ-cyclodextrin) positions. Each circle represents one glucose unit of the cyclodextrin macrocycle while the yellow circles represent glucose units connected with disulfide bonds. Due to lower symmetry of β-cyclodextrin macrocycle two dimeric products (denoted as β−β and β−β′, respectively) may arise.

[†] IOCB AS CR.
[‡] Charles University.

(1) Connors, K. A. *Chem. Rev.* **1997**, *97*, 1325–1357.
(2) Rekharsky, M. V.; Inoue, Y. *Chem. Rev.* **1998**, *98*, 1875–1917.
(3) Dodziuk, H. *Cyclodextrins and Their Complexes*; Wiley-VCH: Weinheim, 2006.
(4) Houk, K. N.; Leach, A. G.; Kim, S. P.; Zhang, X. Y. *Angew. Chem., Int. Ed.* **2003**, *42*, 4872–4897.

10.1021/jo802139s CCC: $40.75
Published on Web 12/29/2008

SCHEME 1. Synthesis of Duplex α-Cyclodextrin Doubly Bridged with Disulfide Bonds[a]

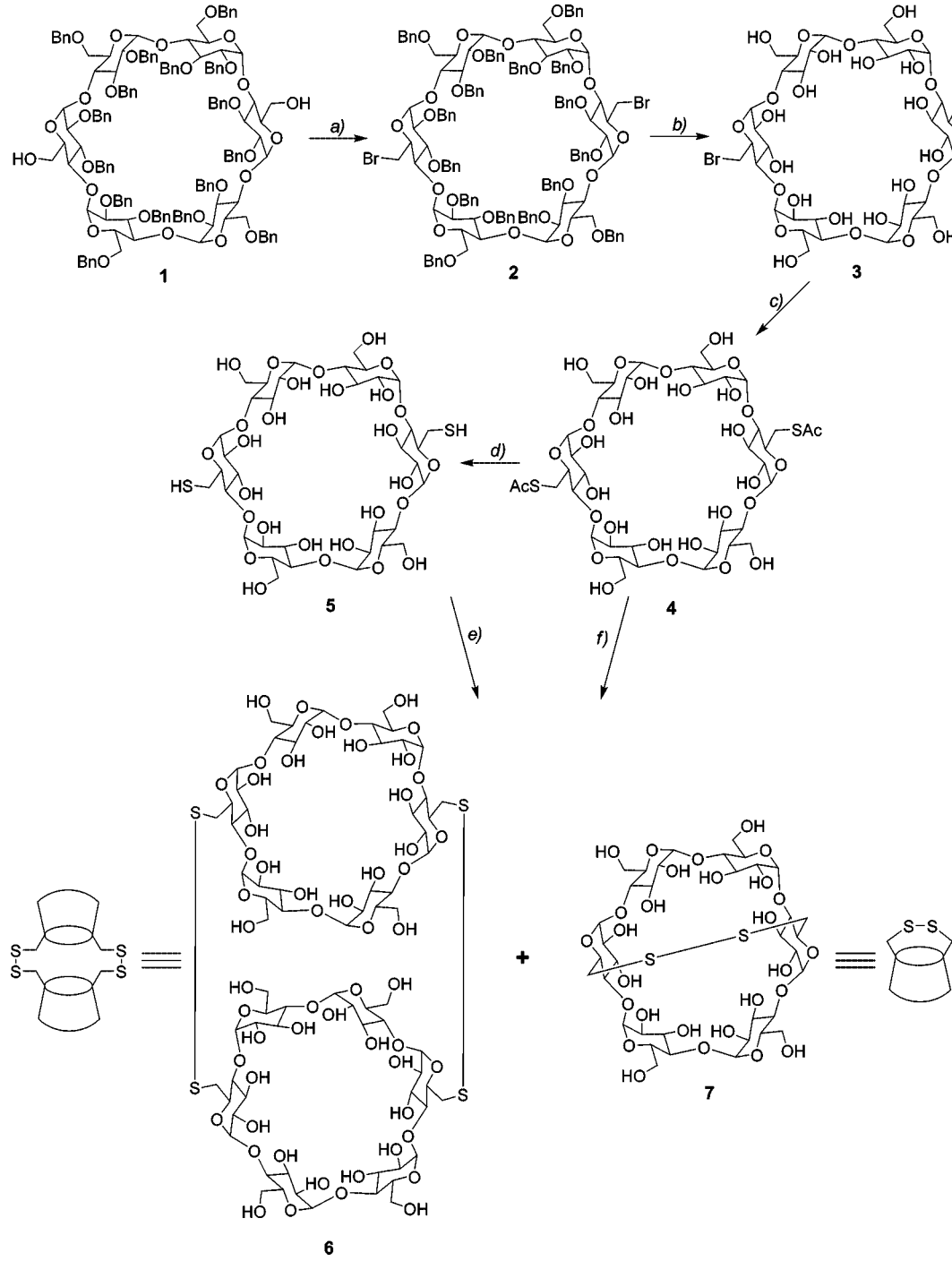

[a] Key: (a) CBr_4, Ph_3P, DMF, 60°C, 95%; (b) Pd/C, 40 barr, DMF−EtOH, rt, 92%; (c) CH_3COSK, DMF, rt, 92%; (d) 1 M NaOH, MeOH−H_2O, rt, 89%; (e) $NaHCO_3$−Na_2CO_3 aq buffer, 10% MeOH, air atmosphere, 87%; (f) (1) 1 M NaOH, MeOH−H_2O; (2) $NaHCO_3$−Na_2CO_3 aq buffer, 10% MeOH, air atmosphere, 91%.

dissociated by more than 99%). Since the binding affinity is assumed to be proportional to the buried surface area of the guest[4] much effort has been devoted to bridging of two cyclodextrin units.[5,6]

In principle, such a coupling can be accomplished by linkers bridging the primary or secondary rims. In several singly bridged β-cyclodextrin dimers remarkably high binding constants were observed,[7,8] while in other instances the two cavities acted in a noncooperative manner giving rise to complexes with stoichiometries 1:2 and displaying usual binding constants.[9] Attempts[10] to freeze the rotational freedom of the two macrocycles by the

(5) Liu, Y.; Chen, Y. *Acc. Chem. Res.* **2006**, *39*, 681–691.
(6) Sliwa, W.; Girek, T.; Koziol, J. J. *Curr. Org. Chem.* **2004**, *8* (15), 1445–1462.
(7) Breslow, R.; Zhang, B. L. *J. Am. Chem. Soc.* **1996**, *118*, 8495–8496.
(8) Breslow, R.; Greenspoon, N.; Guo, T.; Zarzycki, R. *J. Am. Chem. Soc.* **1989**, *111*, 8296–8297.
(9) Liu, Y.; Yang, Y. W.; Yang, E. C.; Guan, X. D. *J. Org. Chem.* **2004**, *69*, 6590–6602.
(10) Tabushi, I.; Kuroda, Y.; Shimokawa, K. *J. Am. Chem. Soc.* **1979**, *101*, 1614–1615.

introduction of an additional linkage were, however, hampered due to the lack of reliable synthetic protocols that would allow selective functionalization in the desired positions. Breslow and Chung synthesized a dimer in which two β-cyclodextrin macrocycles were connected with two different spacers in "vicinal" ($C6^{I}$ and $C6^{II}$) positions.[11] Two stereoisomers termed "aversive" and "oclusive" were isolated of which the latter was shown to form highly stable complexes with shape-compatible guests with binding constants up 10^{10} M^{-1}. Recently, novel synthetic methods[12] allowing highly selective discrimination of two primary hydroxyl groups at $C6^{I}$ and $C6^{IV}$ positions at the cyclodextrin macrocycles opened access also to the synthesis[13−16] of the elusive "transannular" duplexes. However, none of the products designed so far exhibited enhanced complexation.

As a part of our continuing interest[17,18] in multifaceted cyclodextrin chemistry, we have recently focused attention to the duplex cyclodextrins connected with multiple disulfide bridges restricting the rotational freedom of the two macrocycles constituting the host molecule. The disulfide bonds combine several highly desirable properties for the duplex design. They allow—due to the intrinsic capability of a reversible cleavage—generation of dynamic libraries.[19−21] Conceivably, e.g., seven virtual dimeric species (four homodimers and three heterodimers, Figure 1) can be envisaged to arise starting from a mixture of disulfanil derivatives of α-, β-, and γ-cyclodextrins. At the same time, formation of the best binding host for a particular guest could be amplified using the guest molecule as a template. Importantly, the disulfide bond allows to be cleaved also by naturally abundant thiols (glutathione) via thiol−disulfide exchange, which could be exploited in the controlled release of the guest in the targeted drug delivery.

In this introductory paper, we report the efficient synthesis of the duplex cyclodextrin **6** composed of two α-cyclodextrins (α−α dimer in Figure 1) bridged by two disulfide bonds connecting "transannular" $C6^{I}-C6^{I'}$ and $C6^{IV}-C6^{IV'}$ positions. At the same time, we describe the thermodynamic parameters of the formation of inclusion complexes of **6** with a series of α,ω-alkanediols and 1-alkanols in aqueous solutions, and we compare them with those of the analogous singly bridged dimer **10**. The experimental results are complemented with theoretical calculations on a DFT-D level.

Results and Discussion

Synthesis. Compound **1**, prepared by highly selective DIBAL-H-promoted debenzylation[12] of the perbenzylated α-cyclodextrin, was used as a starting material (Scheme 1). Free hydroxylic groups of **1** were converted to bromides by action of triphenylphosphane and tetrabromomethane in DMF, and the corresponding dibromide **2** was isolated in 95% yield. Subsequently, the protecting benzyl groups were removed by hydrogenation using palladium on charcoal as a catalyst. Under controlled conditions (40 bar, 4 h, room temperature), the reaction proceeded cleanly without hydrogenolysis of the bromide groups allowing the isolation of compound **3** in 92% yield. Reaction of dibromide **3** with potassium thioacetate in DMF at room temperature gave rise to the acetylated disulfanil derivative **4** in 92% yield. Subsequent alkaline hydrolysis of **4** under argon atmosphere allowed isolation of the key disulfanil derivative **5** in 89% yield.

The air-oxidation of **5** may, in principle, give rise to a blend of products involving the intramolecular disulfide as well as the corresponding dimeric, oligomeric, and polymeric products. Assuming that the initial concentration of **5** may influence the product distribution, we carried out three experiments at concentrations of 5×10^{-3} M (solubility limit), 10^{-3} M, and 10^{-4} M of **5** in vigorously stirred 50 mM ammonium acetate buffer solution at pH 9.0 in open vials. After completion of the reaction (48 h, ambient temperature), the solution was acidified with acetic acid to pH ~6 and freeze-dried, and the residual ammonium acetate was removed in high vacuum at room temperature.

The ^{1}H NMR spectra recorded under conditions allowing quantitative analysis[22] along with mass spectra established the exclusive formation of only two products identified as the dimer **6** and intramolecular disulfide **7**, respectively (Figure 2). Calculation of their molar ratios in the individual reaction runs revealed that at the lowest concentration (10^{-4} M, Figure 2a) the intramolecular disulfide **7** predominates (91:9), whereas the dimeric product **6** prevails (15:85) at the upper concentration extreme (5×10^{-3} M, Figure 2c). Notably, no other products corresponding to linear open dimers or higher cyclic or linear oligomers were detected in the reaction mixture in this concentration range. Provided that the thiol−disulfide exchange proceeds simultaneously with the oxidation reaction at sufficiently high rate, the apparent equilibrium constant K (eq 1) can be calculated. The obtained values of K (entries 1−3 in Table 1) were, however, found to increase gradually with increasing concentration.

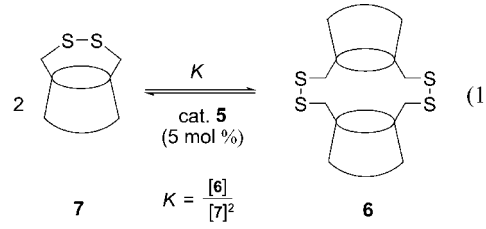

These observations strongly suggest that the reaction proceeded—at least in part—under kinetic control. To impose a thermodynamic control, a series of experiments was carried out starting from the individual products **6** and **7**, respectively, in which the thiol−disulfide exchange was promoted using thiol **5** as a catalyst under *inert atmosphere*. Thus, thiol **5** (5 mol %) was added to the solutions of dimer **6** (entry 4 in Table 1) in deoxygenated 50 mM ammonium acetate buffer at pH 9, and the reaction mixtures were allowed to re-

(11) Breslow, R.; Chung, S. *J. Am. Chem. Soc.* **1990**, *112*, 9659–9660.
(12) Lecourt, T.; Herault, A.; Pearce, A. J.; Sollogoub, M.; Sinay, P. *Chem.—Eur. J.* **2004**, *10*, 2960–2971.
(13) Bistri, O.; Lecourt, T.; Mallet, J. M.; Sollogoub, M.; Sinay, P. *Chem. Biodiversity* **2004**, *1*, 129–137.
(14) Lecourt, T.; Mallet, J.-M.; Sinay, P. *Eur. J. Org. Chem.* **2003**, *455*, 3–4560.
(15) Dong, D. X.; Baigl, D.; Cui, Y. L.; Sinay, P.; Sollogoub, M.; Zhang, Y. M. *Tetrahedron* **2007**, *63*, 2973–2977.
(16) Bistri, O.; Mazeau, K.; Auzély-Velty, R.; Sollogoub, M. *Chem.—Eur. J.* **2007**, *13*, 8847–8857.
(17) Kraus, T.; Buděšínský, M.; Císařová, I.; Závada, J. *Angew. Chem., Int. Ed.* **2002**, *41*, 1715–1717.
(18) Kraus, T.; Buděšínský, M.; Císařová, I.; Závada, J. *J. Org. Chem.* **2001**, *66*, 4595–4600.
(19) Otto, S.; Furlan, R. L. E.; Sanders, J. K. M. *J. Am. Chem. Soc.* **2000**, *122*, 12063–12064.
(20) West, K. R.; Bake, K. D.; Otto, S. *Org. Lett.* **2005**, *7*, 2615–2618.
(21) Corbett, P. T.; Leclaire, J.; Vial, L.; West, K. R.; Wietor, J. L.; Sanders, J. K. M.; Otto, S. *Chem. Rev.* **2006**, *106*, 3652–3711.
(22) Pauli, G. F.; Jaki, B. U.; Lankin, D. C. *J. Nat. Prod.* **2005**, *68*, 133–149.

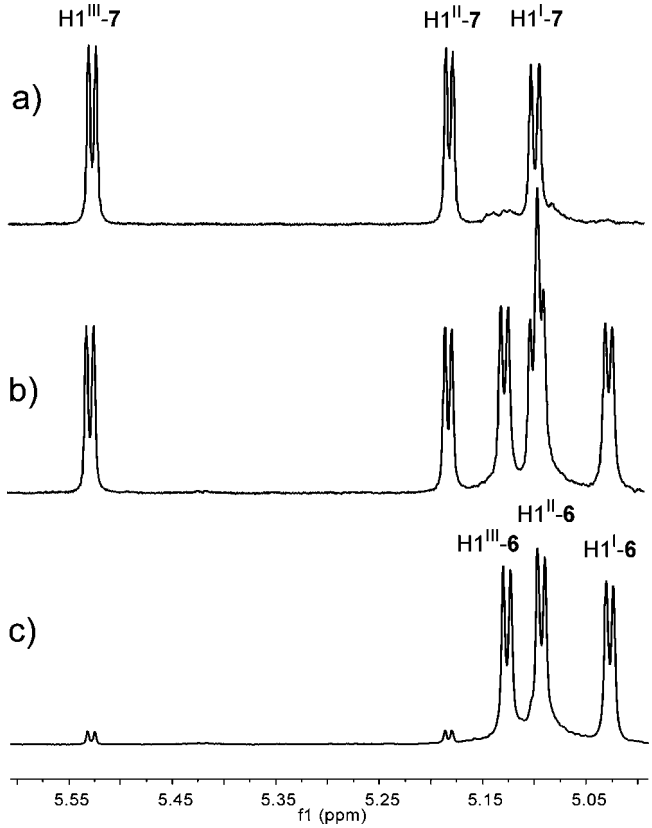

FIGURE 2. Parts of ^{1}H NMR spectra (D_2O; 600 MHz) showing H-1 protons of dimer **6** and intramolecular disulfide **7** in reaction mixtures at various initial concentrations of **5**: (a) 10^{-4} M; (b) 10^{-3} M; (c) 5×10^{-3} M.

equilibrate for 48 h under argon atmosphere. Then the solutions were worked up as described above and the molar ratios of **6** and **7** were determined by quantitative ^{1}H NMR. Analogous equilibrations were also carried out starting from the intramolecular disulfide **7**. These equilibration experiments yielded a consistent set of equilibrium constants (average 1.9×10^4 M^{-1}) clearly demonstrating that the dimer **6** is the *thermodynamically favored product* in the investigated concentration range.

Composition of products in thermodynamically driven reactions can also be controlled by addition of a suitable template which stabilizes certain species by formation of a complex. The use of a template in the dimerization of **5** is a challenging option to amplify the formation of dimer **6** in the reaction mixture even at low concentrations. Molecular modeling revealed that aliphatic hydrocarbon chains longer than 10 carbon atoms should fit into the dimer **6**. Among various α,ω-bifunctional derivatives of alkanes tested, 1,16-hexadecanedioic acid proved the most suitable template providing the required solubility of the complex in alkaline solution. Thus, thiol **5** was added to a buffered aqueous solution (entry 5 in Table 1) containing suspended 1,16-hexadecanedioic acid (0.5 mol equiv). Although the template itself turned out to be poorly soluble, it dissolved completely within 20 min after the addition of **5**. Monitoring of the reaction mixture by reversed-phase TLC revealed the formation of a single product within 24 h. The product, whose structure was determined by NMR analysis to be the inclusion complex of the dimer **6** and 1,16-hexadecanedioic, was isolated in 92% yield by means of precipitation invoked by lowering of pH of the solution. The template could partly be removed from the cavity of the dimer **6** by reversed-phase chromatography in the acetonitrile−water system, the yield of free dimer **6** being highly dependent on the sample/phase ratio as well as on the flow rate parameters.

Given the difficulties encountered in removing 1,16-hexadecanedioic acid from the complex in the templated version of the dimerization reaction, we sought an optimization of the template-free preparative procedure. It was found that an even more favorable ratio of **6** vs **7** could be obtained when the oxidation of **5** was carried out in aqueous sodium carbonate buffer (pH 9) containing 10% of methanol (entry 6 in Table 1). After the completion of the reaction, the ^{1}H NMR analysis revealed the presence of **6** and **7** in molar ratio 93:7. Consequently, the dimer **6** was isolated by reversed-phase chromatography in 87% yield. Importantly, a one-pot oxidation could also be accomplished in excellent yield starting from thioacetate **4**; first the hydrolysis of the acetyl groups with 1 M aqueous NaOH under argon atmosphere was carried out followed by air oxidation after the basicity of the reaction mixture was adjusted to pH 9 with solid carbon dioxide.

In addition to the doubly bridged duplex cyclodextrin **6**, we have synthesized its singly bridged analogue **10** (Scheme 2) as a reference compound for physicochemical studies (vide infra). The starting 6-bromo-6-deoxy-α-cyclodextrin **8** was prepared by reaction of α-cyclodextrin with 6-fold excess of tetrabromomethane and triphenylphosphane at 40 °C in 31% yield. Next, it was converted to thioacetate **9** in 89% yield using the same protocol as described for **4**. Dimer **10** was obtained in 80% yield in a one-pot reaction by alkaline hydrolysis of **9** followed with air oxidation under conditions analogous to those used for the preparation of **6**.

Structure Analysis. The structures of compounds **1**−**10** were confirmed by mass as well as ^{1}H and ^{13}C NMR spectra. The expected C_2-symmetry of compounds **1**−**7** is evidenced by the presence of three sets of signals in NMR spectra (glucose residues I and IV, II and V, and III and VI are symmetrically equivalent), whereas C_1-symmetry (six sets of signals) is observed for compounds **8**−**10**. Structural identity of four or even five glucose residues (II, III, V, VI in **1**−**7**; II−VI in **8**−**10**) results in complex NMR spectra due to the partial overlap of H-2, H-3, H-4 and H-5 signals for slightly chemically nonequivalent glucose residues. Yet, the complete structural assignment including the positions of the individual glucose residues in cyclodextrin ring was successfully accomplished for compounds **1**−**7**. For compounds **8**−**10** having six nonequivalent glucose residues, only signals of the specifically C-6 substituted residue (I) were completely assigned while for the others the sequential assignment (II−VI) is either partial or remains undetermined (see Tables S1 and S2 in the Supporting Information).

The observed multiplicities of hydrogen signals and their coupling constants (J(1,2) ∼ 3.5 Hz, J(2,3) ∼ J(3,4) ∼ J(4,5) = 8.5 − 10 Hz) correspond to the α-D-glucopyranose units in the $^4C_1$ conformation (Figure 3a). Coupling constants J(5,6a), J(5,6b), and J(6a,6b) show larger variations depending on the type and orientation of the C-6 substituent.

While in D_2O and CD_3OD the signals of OH protons are not observed (due to the exchange with deuterium), the OH signals in DMSO usually show well-resolved doublets for 2-OH and 3-OH and triplets or doublets of doublets for 6-OH. The values of coupling constants ^3J(CH,OH) are characteristic for the position of OH group: ^3J(H2,OH) = 6.5−7.5 Hz, ^3J(H3,OH)

TABLE 1. Ratios of Dimer 6 and Intramolecular Disulfide 7 under Variable Reaction Conditions

entry	solvent, buffer system	conc[a] (M)	molar ratio of **6**:**7**	K (M^{-1})
1[b]	H_2O, 50 mM CH_3COONH_4, pH 9	10^{-4}	9:91	1.1×10^3
2[b]	H_2O, 50 mM CH_3COONH_4, pH 9	10^{-3}	44:56	2.1×10^3
3[b]	H_2O, 50 mM CH_3COONH_4, pH 9	5×10^{-3}	85:15	1.3×10^4
4[c]	H_2O, 50 mM CH_3COONH_4, pH 9	10^{-4} to 5×10^{-3}		$1.9 \times 10^4 \pm 0.2 \times 10^4$
5[d]	H_2O, 50 mM CH_3COONH_4, pH 9	10^{-4}	≥99:1	n.d.
6	H_2O-CH_3OH 9:1, 50 mM $Na_2CO_3-NaHCO_3$, pH 9	4.4×10^{-3}	93:7	2.1×10^4

[a] Concentration of the starting thiol **5** (entries 1−3 and 5, 6) or of the monomeric equivalent **7** (entry 4). [b] In the presence of air oxygen. [c] Average of 10 equilibrations starting from **6** or **7** catalyzed with 5 mol % of thiol **5** under inert atmosphere in the indicated concentration range. [d] Dimerization was carried out in presence of 0.5 molar equiv of 1,16-hexadecanedioic acid with respect to **5**; product was isolated as an inclusion complex.

TABLE 2. Thermodynamic Parameters of the Complex Formation of 6 and 10 with α,ω-Alkanediols and 1-Alkanols

entry	dimer	guest	$K \pm \sigma_K$ (M^{-1})	$\Delta H° \pm \sigma_{\Delta H°}$ (kcal·mol^{-1})	$T\Delta S° \pm \sigma_{T\Delta S°}$ (kcal·mol^{-1})	$\Delta G° \pm \sigma_{\Delta G°}$ (kcal·mol^{-1})
1	**10**	1,11-undecanediol	$1.33 \times 10^5 \pm 3.89 \times 10^3$	-11.75 ± 0.16	-4.76 ± 0.17	-6.99 ± 0.02
2	**10**	1,12-dodecanediol	$1.74 \times 10^6 \pm 4.91 \times 10^4$	-13.11 ± 0.15	-4.60 ± 0.16	-8.51 ± 0.02
3	**10**	1,13-tridecanediol	$8.88 \times 10^6 \pm 1.84 \times 10^5$	-14.81 ± 0.16	-5.33 ± 0.17	-9.48 ± 0.01
4	**10**	1,14-tetradecanediol	$3.15 \times 10^7 \pm 7.28 \times 10^5$	-15.52 ± 0.18	-5.29 ± 0.18	-10.23 ± 0.01
5	**6**	1,9-nonanediol	$1.11 \times 10^5 \pm 1.71 \times 10^3$	-11.51 ± 0.10	-4.63 ± 0.11	-6.88 ± 0.01
6	**6**	1,10-decanediol	$2.23 \times 10^6 \pm 6.63 \times 10^4$	-14.34 ± 0.15	-5.68 ± 0.16	-8.66 ± 0.02
7	**6**	1,11-undecanediol	$2.96 \times 10^7 \pm 6.82 \times 10^5$	-16.44 ± 0.18	-6.25 ± 0.18	-10.19 ± 0.01
8	**6**	1,12-dodecanediol[a]	$4.86 \times 10^8 \pm 2.51 \times 10^7$	-18.05 ± 0.21	-6.20 ± 0.23	-11.85 ± 0.03
9	**6**	1,13-tridecanediol[a]	$2.54 \times 10^9 \pm 1.25 \times 10^8$	-19.57 ± 0.22	-6.74 ± 0.24	-12.83 ± 0.03
10	**6**	1,14-tetradecanediol[a]	$8.59 \times 10^9 \pm 3.76 \times 10^8$	-20.32 ± 0.23	-6.77 ± 0.25	-13.55 ± 0.03
11	**6**	1-nonanol	$2.07 \times 10^6 \pm 4.29 \times 10^4$	-11.32 ± 0.13	-2.70 ± 0.14	-8.62 ± 0.01
12	**6**	1-decanol	$2.14 \times 10^7 \pm 5.45 \times 10^5$	-14.42 ± 0.16	-4.42 ± 0.17	-10.00 ± 0.02

[a] Determined by competitive ligand (**10**) binding experiment.

= 2.5−3.5 Hz and ^3J(H6,OH) = 4.7−6.5 Hz (Figure 3b). Thus, the well resolved signals of OH protons were used in identification of signals of individual residues since they offer additional traces in 2D-H,H-TOCSY spectra. The OH signals in DMSO could be identified: (a) by the absence of H/C cross-peaks in 2D-H,C-HSQC spectra, (b) by an upfield shift upon an increase of temperature (c) by exchange with deuterium after addition of small amount of CD_3COOD which removes OH signals along with strong signals of water and reduces multiplicities of H-2, H-3, and H-6 signals. Unfortunately, the distribution of non-exchangeable CH-O signals in DMSO is usually somewhat worse than in D_2O.

The structural assignment of hydrogen signals of individual glucose residues started from H-1 (or OH signals) in the low-field region of 2D-H,H-COSY spectra. The partial overlap of signals H-2, H-3, H-4, and H-5 was solved using 2D-H,H-TOCSY spectra.

Singlet character and larger scale chemical shifts significantly improve the resolution of signals in ^{13}C NMR spectra. Although the chemical shifts of carbon signals in certain position of individual residues often differ only by about 0.01 ppm, the complete overlap of two signals rarely occurred. The characteristic chemical shifts, multiplicities, and namely experimental correlation to directly bonded protons in 2D-H,C-HSQC spectra were used for structural assignments of carbon signals.

After the assignment of hydrogen and carbon signals within glucose units, the positions of glucose units in α-cyclodextrin ring (that is the determination of glucose residues sequence within the macrocycle) were determined either via NOE contacts between H-1 and H-4 of the neighboring residues (it requires sufficient resolution of the corresponding protons) or more frequently via three-bond couplings between H-1/C-4 and H-4/C-1 of the neighboring residues observed as cross-peaks in 2D-H,C-HMBC spectra (Figure 4). Substituent in position 6 (−Br, $-SCOCH_3$, −SH, or −S−) significantly influences the chemical shift of the corresponding C-6 and could be used as a marker for a given residue.

The unequivocal structural evidence for dimer **6** comes from its crystal structure. The single crystals obtained by crystallization of **6** from hot water were submitted to X-ray analysis. The solution of the crystal structure was complicated by a static disorder of cyclodextrin dimers over two positions. Consequently, the site symmetry of the space group of the crystal and the symmetry of the molecule itself did not fit into each other. The outcome of the solution by direct methods was an image consisting, in effect, of two superimposed dimers related by C_2 axis both with occupancies 0.5. This image was dissected into two structures and refined using restrained bond lengths and angles known from a crystal structure of the native α-cyclodextrin.[23]

Inspection of the structure of **6** (Figure 5) reveals that one of the two disulfide bonds is in nearly ideal conformation, the dihedral angle being 93°, whereas the other one is disordered over two positions with about equal occupancy and the respective dihedral angles 110° (Figure 5a) and 119° (Figure 5b). In a view of potential use of the dimer as a host molecule for complexation of various organic molecules, the dimensions of the cavity are of utmost interest. Thus, the maximal length of the dimer expressed as the mean internuclear distance between the most proximal oxygen atoms of the hydroxylic groups located at the opposite peripheries of the dimer (regardless of their assignment to particular glucose units) amounts to 13.7 Å. Analogous calculation for H-3 protons, more relevant to the binding phenomena, yields the effective length 12.1 Å. The width of the dimer is analogous to that of the parent α-cyclodextrin, the narrowest part (∼6.7 Å) being delimitated by disulfide bonds.

Inclusion Complexes. Preliminary molecular modeling based on the cavity dimensions (vide supra) suggested that the dimer **6** should effectively bind compounds containing linear aliphatic

SCHEME 2. Synthesis of α-Cyclodextrin Dimer Singly Bridged with a Disulfide Bond [a]

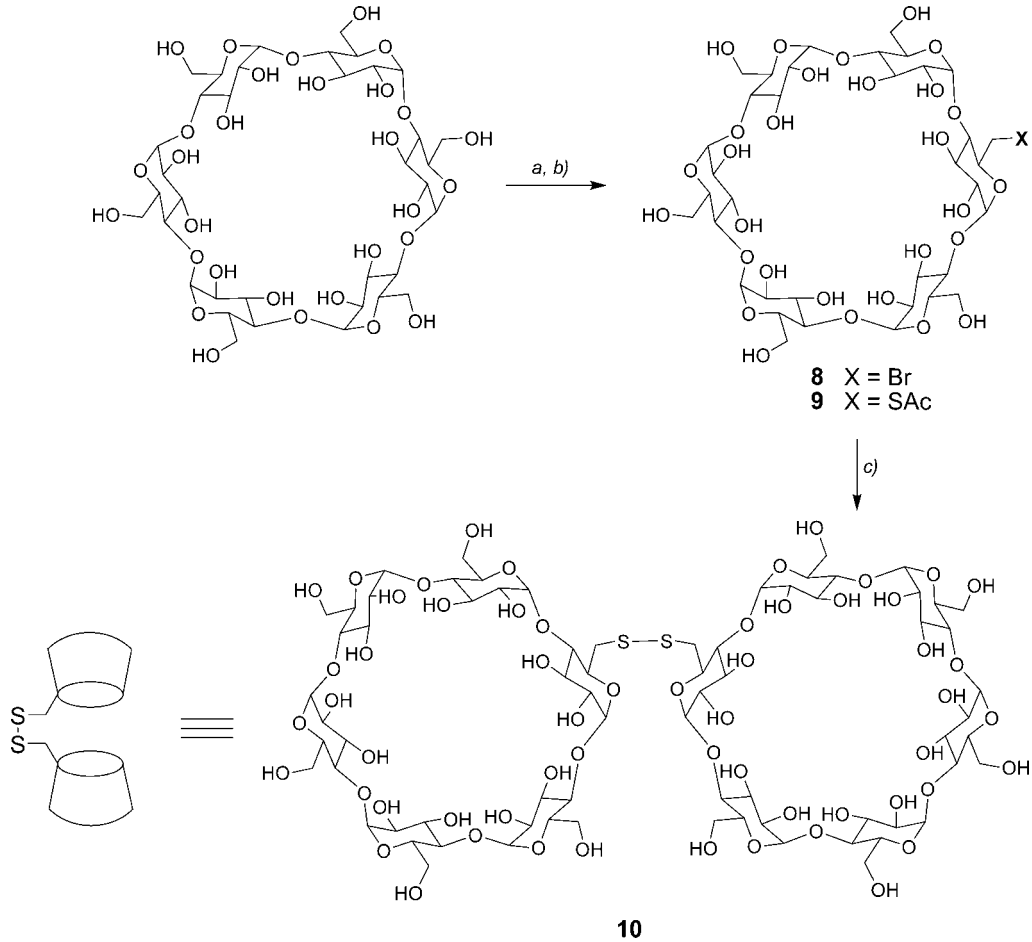

[a] Key: (a) CBr_4, Ph_3P, DMF, 40 °C, 31%; (b) CH_3COSK, DMF, rt, 89%; (c) (1) 1 M NaOH, MeOH−H_2O, rt; (2) $NaHCO_3$−Na_2CO_3 aq buffer, 10% MeOH, air atmosphere, 80%.

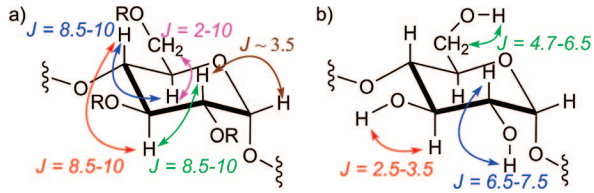

FIGURE 3. Observed values of vicinal proton couplings in cyclodextrin derivatives **1**−**10**: (a) ^3J(H,H); (b) ^3J(H,OH).

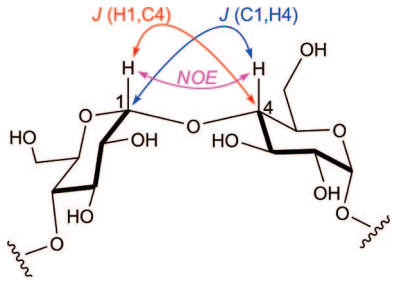

FIGURE 4. Schematic diagram of the sequential assignment of glucose residues using 2D-H,H-ROESY (NOE contact between H-1 and H-4 of neighboring residues) and 2D-H,C-HMBC spectra (cross-peaks corresponding to ^3J(H1,C4) and ^3J(C1,H4) of neighboring residues).

alkyl chains. Thus, we have chosen a set of α,ω-alkanediols (C_9−C_{14}) and 1-alkanols (C_9 and C_{10}) as model compounds to investigate the ability of the dimer **6** to form inclusion complexes. The reactions were studied by isothermal titration calorimetry (ITC) in aqueous solutions. For the determination of $K \geq 1 \times 10^8$ M^{-1}, competitive titrations[24] using dimer **10** as the weaker ligand were employed.

To ensure reliable reproducibility of the results, the determination of estimates of N, K, and $\Delta H°$ was carried out in series, each consisting of five replicate titrations using the same stock solutions and equal experimental conditions. In line with the recent findings by Tellinghuisen, we have used "one plus ten" injection protocol[25,26] for most of the titrations. The individual titration runs were first evaluated independently to check for outlying results. The final estimates reported in Table 2, however, were obtained by analysis of a single set of preaveraged raw data consisting of all five runs. This approach[27]—analogous to signal accumulation—proved beneficial especially when titrations were done at low concentrations: in most cases, χ^2 values dropped down as compared to the individual titration runs (Supporting Information). The estimates of K, $\Delta H°$, and the respective standard errors σ_K and $\sigma_{\Delta H°}$ were directly obtained by nonlinear least-squares fitting of the one-site model to the experimental binding isotherm using the MicroCal software implemented in Origin 7. Values of estimates of $\Delta G°$ and $T\Delta S°$ were calculated according to eqs 2 and 3, respectively. The corresponding standard errors $\sigma_{\Delta G°}$ and $\sigma_{T\Delta S°}$ were calculated using eqs 4 and 5, respectively (see the Supporting Information for derivations), where $\rho_{K,\Delta H°}$ stands for the correlation coefficient of K and $\Delta H°$ calculated from covariance matrix. In addition, the standard errors reported in

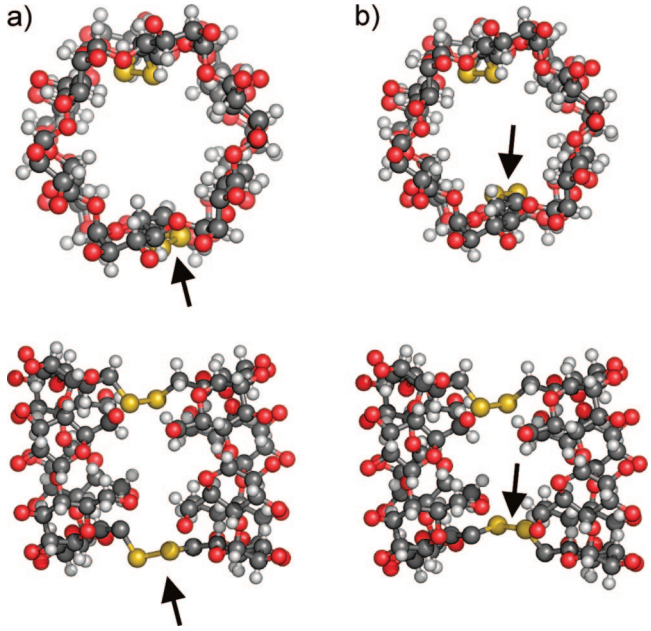

FIGURE 5. Crystal structure of duplex cyclodextrin **6**. Top-down and side views of two conformers differing in positions and dihedral angles [(a) 110°; (b) 119°] of the disordered disulfide bond (indicated by arrows). Spheres represented at 30% of van der Waals radius. Water molecules omitted for clarity. Positions of hydrogens at hydroxylic groups could not be determined.

Table 2 contain the impact of ±1% concentration error of the titrant in the pipet.

$$\Delta G^\circ = -RT \ln K \quad (2)$$

$$T\Delta S^\circ = \Delta H^\circ - \Delta G^\circ \quad (3)$$

$$\sigma_{\Delta G^\circ} = \sqrt{\left(\frac{-RT}{K}\right)^2 \sigma_K^2} \quad (4)$$

$$\sigma_{T\Delta S^\circ} = \sqrt{\sigma_{\Delta H^\circ}^2 + \left(\frac{RT}{K}\right)^2 \sigma_K^2 + 2\left(\frac{RT}{K}\right)\rho_{K,\Delta H^\circ}\sigma_{\Delta H^\circ}\sigma_K} \quad (5)$$

Initial replicate experiments, in which an aqueous solution of 1,10-decanediol was titrated into a solution dimer **6** in the cell, revealed poor reproducibility of the stoichiometric parameter N in the individual titration runs. Typically, the N parameter decreased from run to run by 3−5% while K and ΔH° remained constant within the experimental error. When the titration mode was reversed (solution of the dimer **6** in the pipet), all three estimates of parameters (N, K, ΔH°) changed. This strongly suggested a systematic time-dependent variability in the concentration of the stock solution of the dimer. Indeed, another several sets of experiments, in which different batches of materials as well as glass containers were employed, indicated that both dimers **6** and **10** tend to adsorb to soft amber glass of the vials used for the storage of stock solutions. The problem was solved by using clear borosilicate glass bottles. Screening of the optimal experimental conditions for the titration of 1,10-decanediol with the dimer **6** in neat water and in various buffered solutions (5 mM phosphate buffer pH 7.0 and 6.4; 1 mM citric buffer pH 6.4; 2 mM formic buffer pH 4.0) revealed that neither the presence of a buffer nor the change of pH significantly influence the values of K and ΔH°. Therefore, all measurements were performed in neat degassed water.

Inspection of the binding parameters (Table 2) clearly shows that the binding affinity of the doubly bridged dimer **6** to an

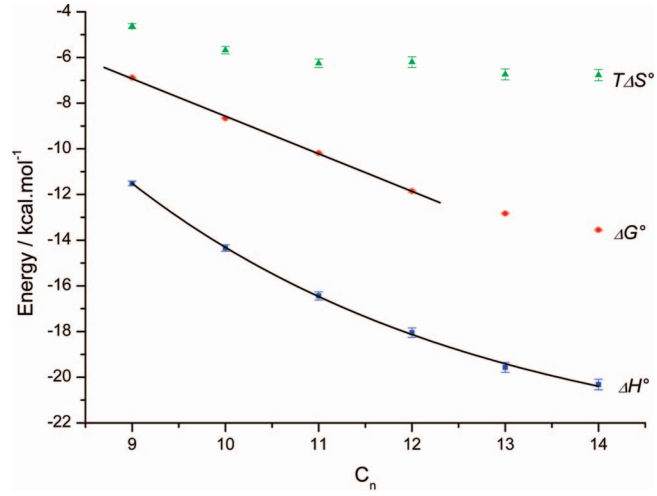

FIGURE 6. Plot of the thermodynamic parameters of binding of the dimer **6** to α,ω-alkanediols in dependence on number of carbon atoms C_n in the alkane chain: green triangles, $T\Delta S^\circ$; red circles, ΔG°; blue squares, ΔH°. Linear and exponential fits of ΔG° and ΔH°, respectively (see text).

α,ω-alkanediol is, in general, higher by about 2 orders of magnitude in K (M^{-1}) or 3.1−3.3 kcal/mol in ΔG° compared to the singly bridged analogue **10**. Dissection of the standard free energy into enthalpic and entropic components reveals that the inclusion process is driven by enthalpy (up to −20.3 kcal/mol for **6**·C_{14} homologue, entry 10) which is partially offset by an entropy loss comparable in both series. The more potent affinity of the doubly bridged dimer **6** thus results mainly from enthalpy gain.

Thermodynamic functions (e.g., solvation energies $\Delta_h G^\circ$ and $\Delta_h H^\circ$) of the homologous series of hydrocarbons and their derivatives very often show linear correlation with the number of methylene units in the chain.[28] Accordingly—and in line with the postulate attributing the overall binding affinity to the buried surface area of the guest[4]—a growing number of methylene groups in the α,ω-alkanediol should favorably contribute to the overall binding up to a certain limit corresponding to the "optimal length" of the hydrocarbon chain. Assuming zigzag conformation of the alkyl chain, 1,11-undecanediol having eleven carbon atoms appears to have that optimal length with respect to the cavity size (mean distance between H-3 and H-3′ protons is ∼12.1 Å). Beyond this length, methylene groups of the hydrocarbon chain would remain outside the dimer cavity exhibiting no contribution to the binding. However, the dependence of thermodynamic parameters on the alkyl chain length for complexes of dimer **6** with α,ω-alkanediols (Figure 6) only partly supports such a simplified view. The standard free energy ΔG° plot reveals linear correlation ($r^2 = 0.999$) for complexes of up to twelve carbon atoms followed by diminished yet still significant energy increments for the "outsized" members of the series (C_{13}, C_{14}). The standard enthalpy change plotted on the same scale exhibits an exponential decrease with growing hydrocarbon chain over the whole series. The curve can be fitted

(23) Chacko, K. K.; Saenger, W. *J. Am. Chem. Soc.* **1981**, *103*, 1708–1715.
(24) Sigurskjold, B. W. *Anal. Biochem.* **2000**, *277*, 260–266.
(25) Tellinghuisen, J. *J. Phys. Chem. B* **2005**, *109*, 20027–20035.
(26) Tellinghuisen, J. *Anal. Biochem.* **2005**, *343*, 106–115.
(27) Turnbull, W. B.; Precious, B. L.; Homans, S. W. *J. Am. Chem. Soc.* **2004**, *126*, 1047–1054.
(28) Plyasunov, A. V.; Shock, E. L. *Geochim. Cosmochim. Acta* **2000**, *64*, 439–468.

into empirical function $y = -23.7 + 127.9\exp(-0.26C_n)$, the extrapolation of which suggests that the maximum achievable enthalpy gain in the series of α,ω-alkanediols approaches a limit of about −24 kcal/mol. The fourteenth methylene unit in the hydrocarbon chain outsizing the cavity by ∼4 Å still adds up to 0.75 and 0.72 kcal/mol in enthalpy and free energy change, respectively.

Similar situation was earlier observed[29,30] also in complexation studies of the parent α-cyclodextrin and attributed to an "expanded hydrophobic sphere".[2] While such an explanation based on solvation effects may be reasonable, the compression of the alkane chain in the cavity by means of helical coiling suggested by Rebek[31,32] et al. in complexation of alkanes by synthetic cavitands of similar dimensions also comes into consideration. Third, principal component analysis of molecular dynamics simulation (vide infra) suggests a considerable rotational freedom about disulfide bonds which may allow a moderate adjustment of the dimer cavity length in dependence on the alkane chain length.

In this context, it is of interest to investigate the role of terminal hydroxylic groups in the thermodynamics of the complexation process. Comparison of thermodynamic parameters of reactions of **6** with 1,9-nonadiol (entry 5) vs 1-nonanol (entry11) and 1,10-decanediol (entry 6) vs 1-decanol (entry 12) reveals that 1-alkanols bind more efficiently to the dimer **6** than the corresponding α,ω-alkanediols by 1.74 and 1.34 kcal/mol of $\Delta G°$ for the former and latter pair, respectively. Interestingly, this enhancement in binding affinity is due to more favorable entropy change.

Molecular Modeling. The binding of α,ω-alkanediols by dimer **6** was also studied by theoretical methods. The goal of the study was to estimate the intrinsic (solute−solute) interactions free from solvation effects using DFT-D methods which properly account for dispersion interactions. Moreover, the most abundant collective vibrational modes of the complex of **6** with 1,10-decanediol were identified by principal component analysis (PCA) of molecular dynamics (MD) simulation in explicit solvent.

Since the crystal structure of the dimer **6** was not available at the beginning of the study, the initial model was built using coordinates of the known crystal structure[23] of the parent α-cyclodextrin. The structure of **6** was subjected to MD simulation, the equilibrated structure was optimized by empirical methods and further optimized using RI-DFT-D method[33] (see the Supporting Information for a more detailed description of the procedures). It should be noted that the model structure thus obtained is consistent with that revealed by crystal structure analysis of dimer **6** later in the course of the study. A series of six inclusion complexes of dimer **6** and α,ω-alkanediols (C_9−C_{14}) was built with constraints reflecting the shape and topological parameters of the cavity of dimer **6**. The ligands were docked into the cavity of the **6**, and their initial positions were adjusted by molecular mechanics optimization utilizing the Cornell force field[34] for further calculations. The complex was then solvated by approximately 1635 molecules of SPC water,[35] equilibrated for 100 ps and subjected to 1 ns MD simulation with periodic boundary conditions. Ten structures of the lowest energy for each complex were chosen along the MD trajectory and energetically minimized using the Cornell force field[34] including positions of all water molecules. The structure with the lowest potential energy was selected and analyzed by RI-DFT-D method to obtain the energy characteristics of the binding, water molecules being excluded from the interaction energy evaluation. The total interaction energy was calculated as the energy difference between energy of the **6**·diol complex and a sum of energies of the isolated diol and dimer **6**.

TABLE 3. Calculation of Interaction Energies for the Complexes of 6 and α,ω-Alkanediols

	RI-DFT-D (TPSS/TZVP)		SCC-DFTB-D, (gas phase)	
no. of methylene groups	D_{int}[a] (kcal/mol)	Total energy (kcal/mol)	D_{int}[a] (kcal/mol)	Total energy (kcal/mol)
9	−48.91	−45.13	−50.75	−44.20
10	−50.64	−46.39	−53.56	−44.07
11	−55.29	−56.51	−58.14	−54.55
12	−57.29	−53.78	−60.31	−51.74
13	−59.18	−58.09	−61.12	−53.06
14	−59.21	−56.61	−62.61	−57.60

[a] D_{int}: separated dispersion energy term.

In order to evaluate the influence of the surrounding water molecules on the optimization procedure, the system with excluded water molecules was then again subjected to gradient optimization (gas phase) using the self-consistent charges density functional tight binding method (SCC-DFTB-D) augmented with the empirical dispersion term.[36] Then the interaction energy of the optimized complexes was recalculated at the resolution of identity density functional theory including the dispersion correction RI-DFT-D. Comparison of the results obtained by the two approaches (Table 3) suggests only a moderate effect of the aqueous medium on the optimization procedure.

Separation of the dispersion term (D_{int}) from the total interaction energy indicates that dispersion interactions are the driving force of the process. In the light of these findings, it is of interest to re-examine the concept[37] of "enthalpy-rich" cavity-bound water molecules as a driving force for the complexation. The complete thermodynamic cycle can be expressed in terms of enthalpy contributions (eq 6) where $\Delta_h H_{\mathbf{6}}$, $\Delta_h H_D$, and $\Delta_h H_{\mathbf{6}\cdot D}$ stand for hydration enthalpies of the dimer **6**, the diol and the complex **6**·diol, respectively. The term ΔH_i represents the intrinsic (solute−solute) enthalpy, which is relevant to the calculated interaction energies, and ΔH_{exp} is the experimentally observed enthalpy of reaction (Table 2). The hydration enthalpies of α,ω-alkanediols can be estimated using group additivity methods[28,38] (values range from −27.6 to −32.1 kcal/mol for 1,9-nonanediol and 1,14-tetradecanediol, respec-

(29) Bastos, M.; Briggner, L. E.; Shehatta, I.; Wadso, I. *J. Chem. Thermodyn.* **1990**, *22*, 1181–1190.
(30) Hallen, D.; Schon, A.; Shehatta, I.; Wadso, I. *J. Chem. Soc., Faraday Trans.* **1992**, *88*, 2859–2863.
(31) Scarso, A.; Trembleau, L.; Rebek, J. *Angew. Chem., Int. Ed.* **2003**, *42*, 5499–5502.
(32) Scarso, A.; Trembleau, L.; Rebek, J. *J. Am. Chem. Soc.* **2004**, *126*, 13512–13518.
(33) Jurecka, P.; Cerny, J.; Hobza, P.; Salahub, D. R. *J. Comput. Chem.* **2007**, *28*, 555–569.
(34) (a) Cornell, W. D.; Cieplak, P.; Bayly, C. I.; Gould, I. R.; Merz, K. M.; Ferguson, D. M.; Spellmeyer, D. C.; Fox, T.; Caldwell, J. W.; Kollman, P. A. *J. Am. Chem. Soc.* **1995**, *117*, 5179–5197. (b) Cornell, W. D.; Cieplak, P.; Bayly, C. I.; Gould, I. R.; Merz, K. M.; Ferguson, D. M.; Spellmeyer, D. C.; Fox, T.; Caldwell, J. W.; Kollman, P. A. *J. Am. Chem. Soc.* **1996**, *118*, 2309–2309.
(35) Reddy, M. R.; Berkowitz, M. *Chem. Phys. Lett.* **1989**, *155*, 173–176.
(36) Elstner, M.; Hobza, P.; Frauenheim, T.; Suhai, S.; Kaxiras, E. *J. Chem. Phys.* **2001**, *114*, 5149–5155.
(37) Bender, M. L.; Komiyama, M. *Cyclodextrin Chemistry*; Springer-Verlag: Berlin, 1978; p 23.
(38) Plyasunov, A. V.; Shock, E. L. *J. Chem. Eng. Data* **2001**, *46*, 1016–1019.

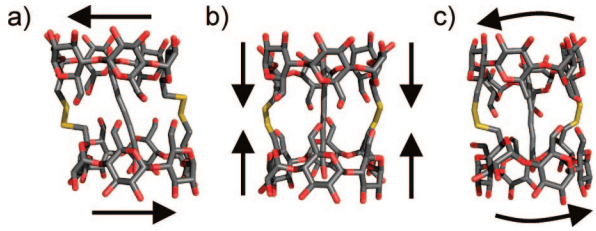

FIGURE 7. First three most pronounced vibrational modes of the complex of **6** with 1,9-nonanediol as identified by PCA: (a) sliding, (b) stretching, and (c) twisting of the cavities caused by the deformation of the disulfide bonds.

tively) whereas hydration enthalpies Δ_hH_6 of the dimer and $\Delta_hH_{\mathbf{6}\cdot D}$ of the complex are unknown. The difference between these two terms (eq 7), however, represents the hydration enthalpy gain/loss as a consequence of the changes of the solvation of dimer **6** upon complexation. Calculations using values of interaction energies of gas-phase optimized complexes (right column in Table 3) as ΔH_i reveal positive values in the range of 1−9 kcal/mol in the examined series. Provided that the single point interaction energy calculations sufficiently represent the real situation, the desolvation of the cavity appears to be retarding rather than the driving force of the reaction.

$$\Delta_hH_{\mathbf{6}} + \Delta_hH_D + \Delta H_{exp} = \Delta_hH_{\mathbf{6}\cdot D} + \Delta H_i \quad (6)$$

$$\Delta_hH_{\mathbf{6}\cdot D} - \Delta_hH_{\mathbf{6}} = \Delta_hH_D + \Delta H_{exp} - \Delta H_i \quad (7)$$

Principal component analysis (PCA) of the dynamics of the complex allows to identify large scale collective motions (vibrational modes) that occur in system. We have used PCA to analyze 5 ns MD simulations of the complex of **6** with 1,9-nonanediol. The first three principle components (modes 1−3, Figure 7a−c) shown in their amplitudes capture the most important distortions of the **6**·diol complex geometry. The first dynamical motion (Figure 7a) causes deformation of dihedral C−S−S−C angles of both disulfide bonds of **6** (101° and 99°, respectively) resulting in mutual shifting of the two α-cyclodextrin cavities along an axis perpendicular to the ideal longitudinal C_2 axis. Interestingly, similar deformation is found in one of the disulfide bonds (disordered over two positions) in the crystal structure of **6**. The other two modes represent the deformation of the molecule of **6** in a puckering-like (Figure 7b) and twisting-like (Figure 7c) manner.

Conclusions

The duplex cyclodextrin **6** composed of two α-cyclodextrin macrocyles held by two disulfide bonds in transannular ($C6^I$, $C6^{IV}$) positions was prepared from partially debenzylated α-cyclodextrin **1** in four steps and 73% overall yield. In the key oxidation step, aside of dimer **6** the intramolecular disulfide **7** forms from the parent thiol as a sole byproduct. The ratio of dimer **6** and intramolecular disulfide **7** could be conveniently directed by the choice of the reaction conditions, in particular by the concentration of the starting thiol. The reversibility of the disulfide bond was demonstrated by an equilibration of either dimer **6** or intramolecular disulfide **7** promoted with a thiol catalyst[39] under inert atmosphere. The structure of duplex cyclodextrin **6** was established by MS and 2-D NMR methods and confirmed by a single-crystal X-ray analysis.

The ability of the duplex cyclodextrin **6** to bind α,ω-alkanediols (C_9−C_{14}) and 1-alkanols (C_9 and C_{10}) was studied by ITC in aqueous solutions. It was found that the doubly bridged dimer **6** exhibits higher binding affinity than its singly bridged analogue **10** by about 2 orders of magnitude in K (M^{-1}) or 3.1−3.3 kcal/mol in $\Delta G°$ as a consequence of enthalpic factors. The stability constant of the complex of dimer **6** with 1,14-tetradecanediol reaches 8.6×10^9 M^{-1}, which is an unprecedently high value for α-cyclodextrin complexes reported to date.

The source of the binding affinity was investigated by theoretical calculation (DFT-D method) suggesting that the main enthalpic gain comes from dispersion interactions whereas the solvation effects appear to be destabilizing factors.

The duplex α-cyclodextrin, due to its high binding affinity toward shape-compatible guests, is envisaged to find versatile application in the design of rotaxanes and catenanes in aqueous solution. Due to the reversibility of the disulfide bonds, analogous larger duplexes constructed from β- and γ-cyclodextrins may serve as interesting host molecules for targeted drug delivery. Such studies are currently underway in our laboratory.

Experimental Section

General experimental methods along with chemical shifts of ^1H and ^{13}C NMR spectra (Tables S1 and S2, respectively) can be found in the Supporting Information. Satisfactory elemental analysis could not be obtained for compounds **3**−**10** unless variable numbers of water molecules were taken into account. Thus, calculations based on weights of these compounds (molarity, yield, optical rotation) are related to the hydrated molecules.

2^I, 2^{II}, 2^{III}, 2^{IV}, 2^V, 2^{VI}, 3^I, 3^{II}, 3^{III}, 3^{IV}, 3^V, 3^{VI}, 6^{II}, 6^{III}, 6^V, 6^{VI}-Hexadeca-*O*-benzyl-6^I,6^{IV}-dibromo-6^I,6^{IV}-dideoxy-α-cyclodextrin 2. Triphenylphosphane (1.309 g, 5.0 mmol) and tetrabromomethane (1.66 g, 5.0 mmol) were dissolved in dry DMF (5.4 mL) in a Schlenk flask under argon atmosphere, and compound **1** (2.02 g, 0.837 mmol) was added subsequently. The reaction mixture was heated to 60 °C for 12 h, and then the reaction was quenched by addition of MeOH (1 mL). The mixture was allowed to cool to room temperature and diluted with toluene (500 mL). The organic phase was washed with water (3 × 300 mL) and brine (300 mL). Then it was separated and dried with sodium sulfate followed with evaporation. The crude product was purified by column chromatography (500 g silica, isocratic elution with toluene−acetone 99:1). The product was isolated as colorless amorphous material (2.01 g, 95%). For compound **2**: R_f 0.4, toluene−acetone 97:3; $[\alpha]^{20}_D$ = +39 (c = 0.3 in $CHCl_3$); ^1H NMR, see Table S1 (Supporting Information); ^{13}C NMR, see Table S2 (Supporting Information); MS (ESI) calcd for $C_{148}H_{154}Br_2O_{28}$ $[M + Na]^+$ m/z 2563.9, found 2563.9. Anal. Calcd for $C_{148}H_{154}Br_2O_{28}$: C, 69.97; H, 6.11. Found C, 69.63; H, 6.33.

6^I,6^{IV}-Dibromo-6^I,6^{IV}-dideoxy-α-cyclodextrin 3. Compound **2** (1.270 g, 0.50 mmol) was dissolved in 40 mL of a degassed mixture of DMF−ethanol (1:1). Then palladium on charcoal (10% w/w, 350 mg) was added, and the reaction mixture was placed into an autoclave equipped with a magnetic stirring bar. The autoclave was flushed with argon and filled with hydrogen to a pressure of 40 bar. After the reaction mixture was stirred for 4 h at room temperature, the excessive hydrogen was released and the catalyst was removed from the reaction mixture by filtration through Celite. The solvents were evaporated under reduced pressure. The residue was dissolved in 40 mL of a hot mixture of methanol−water (2:8) and charged onto a C-18 reversed-phase column (25 g, prepared

(39) Aside from the starting thiol **5**, preliminary experiments in our laboratory show that L-glutathione is capable to cleave the free dimer **6**; unfortunately, the low solubilities of the complexes of **6** with α,ω-alkanediols precluded more detailed NMR studies.

in methanol−water 5:95). Gradient elution from methanol−water 5:95 to 40:60 allowed isolation of **3** as white crystalline material (0.530 g, 92%, calcd for trihydrate). For compound **3**: R_f 0.3, RP, methanol−water 4:6; $[\alpha]^{20}_D = +124$ ($c = 0.4$ in DMSO); ^{1}H NMR, see Table S1 (Supporting Information); ^{13}C NMR, see Table S2 (Supporting Information); MS (ESI) calcd for $C_{36}H_{58}Br_2O_{28}$ [M + Na]$^+$ *m*/*z* 1121.1, found 1121.1. Anal. Calcd for $C_{36}H_{58}Br_2O_{28}\cdot 3H_2O$: C, 37.51; H, 5.60. Found: C, 37.61; H, 5.63.

$6^I,6^{IV}$-Bis(thioacetyl)-$6^I,6^{IV}$-dideoxy-α-cyclodextrin 4. Compound **3** (336 mg, 0.290 mmol, calcd for trihydrate) was dissolved in dry DMF (5 mL) in a Schlenk flask equipped with a magnetic stirring bar under argon atmosphere. The mixture was degassed by application of vacuum−argon cycle, and a solution of potassium thioacetate (73 mg, 0. 218 mmol) in dry degassed DMF (1 mL) was added dropwise at room temperature. The mixture was allowed to react for 12 h. It was then poured into acetone (100 mL), and the crude product was separated on a sintered glass as a white precipitate. Subsequent purification by column chromatography (C-18 reversed-phase, gradient elution from methanol−water 1: 9 to 3: 7) afforded white microcrystalline material (291 mg, 92%, calcd for trihydrate). For compound **4**: R_f 0.35, RP, methanol−water 4:6; $[\alpha]^{25}_D = +162$ ($c = 0.3$ in H_2O); ^{1}H NMR, see Table S1 (Supporting Information); ^{13}C NMR, see Table S2 (Supporting Information); MS (ESI) calcd for $C_{40}H_{64}O_{30}S_2$ [M + K]$^+$ *m*/*z* 1127.3, found 1127.3. Anal. Calcd for $C_{40}H_{64}O_{30}S_2\cdot 3H_2O$: C, 42.03; H, 6.17; S, 5.61. Found: C, 42.32; H, 6.31; S, 5.65.

$6^I,6^{IV}$-Dideoxy-$6^I,6^{IV}$-disulfanil-α-cyclodextrin 5. Compound **4** (124 mg, 0.109 mmol, calcd for trihydrate) was dissolved in water−methanol 9:1 (7 mL), and the whole mixture was degassed by means of vacuum−argon cycle. A degassed 1 M aqueous solution of sodium hydroxide (0.65 mL; 0.65 mmol) was then added, and the mixture was allowed to react for 6 h at room temperature. Then the solution was acidified with 1 M aqueous HCl to pH 5−6, and the solution was rapidly charged onto an reversed-phase column (prepared in methanol−water 5:95) before precipitation occurred. Gradient elution from methanol−water 5:95 to 50:50 gave **5** as white solid (101 mg, 89%, calcd for dihydrate). For compound **5**: R_f 0.45, RP, methanol−water 1:1; $[\alpha]^{25}_D = +141$ ($c = 0.4$ in DMSO); ^{1}H NMR, see Table S1 (Supporting Information); ^{13}C NMR, see Table S2 (Supporting Information); MS (ESI) calcd for $C_{36}H_{60}O_{28}S_2$ [M + Na]$^+$ *m*/*z* 1027.3, found 1027.3. Anal. Calcd for $C_{36}H_{60}O_{28}S_2\cdot 2H_2O$: C, 41.54; H, 6.20; S, 6.16. Found: C, 41.71; H, 6.11; S, 5.87.

Dimer 6 and Intramolecular Disulfide 7 via Air Oxidation of $6^I,6^{IV}$-Dideoxy-$6^I,6^{IV}$-disulfanil-α-cyclodextrin 5. Compound **5** (184 mg; 1.77×10^{-4} mol, calcd for dihydrate) was dissolved in aqueous 0.05 M $NaHCO_3$−Na_2CO_3 buffer (36 mL; pH = 9.0), and methanol (4 mL) was added. The mixture was vigorously stirred in an open flask for 48 h (until no starting material was detected; RP-TLC, acetonitrile−water 3:7). The volume of the reaction mixture was partly reduced on rotatory evaporater, and the remaining solution was neutralized with 1 M HCl. The solution was charged onto a C-18 reversed-phase column (gradient elution from methanol−water 5:95 to 1:1). Compound **7** (white solid, 5.1 mg, 3%, calcd for tetrahydrate) was eluted first followed with a fraction containing **6** (white crystalline material, 164 mg, 87%, calcd for heptahydrate).

Analytical data for compound **6**: R_f 0.2, RP TLC, acetonitrile−water 3:7; $[\alpha]^{25}_D = +216$ ($c = 0.1$ in H_2O); ^{1}H NMR, see Table S1 (Supporting Information); ^{13}C NMR, see Table S2 (Supporting Information); HR MS (ESI) calcd for $C_{72}H_{116}O_{56}S_4$ [M + Na]$^+$ *m*/*z* 2027.5010, found 2027.5081. Anal. Calcd for $C_{72}H_{116}O_{56}S_4\cdot 7H_2O$: C, 40.56; H, 6.15; S, 6.02. Found: C 40.69; H, 6.09; S, 5.83.

Analytical data for compound **7**: R_f 0.6, RP TLC, acetonitrile−water 3:7. $[\alpha]^{25}_D = +118$ ($c = 0.2$ in H_2O); ^{1}H NMR, see Table S1 (Supporting Information); ^{13}C NMR, see Table S2 (Supporting Information); HR MS (ESI) calcd for $C_{36}H_{58}O_{28}S_2$ [M + Na]$^+$ *m*/*z* 1025.2454, found 1025.2421. Anal. Calcd for $C_{36}H_{58}O_{28}S_2\cdot 4H_2O$: C, 40.22; H, 6.19; S, 5.97. Found: C, 40.04; H, 6.10; S, 5.68.

Dimer 6 via One-Pot Dimerization of $6^I,6^{IV}$-Bis(thioacetyl)-$6^I,6^{IV}$-dideoxy-α-cyclodextrin 4. Compound **4** (116 mg, 0.102 mmol, calcd for trihydrate) was dissolved in water (10 mL), and the solution was deoxygenated by means of triple vacuum−argon cycle. Then a deoxygenated aqueous 1 M solution of sodium hydroxide (1 mL, 1 mmol) was added, and the mixture was allowed to react for 6 h under argon atmosphere. The flask was opened, and water (20 mL) and methanol (2 mL) were added to the mixture. The pH of the solution was adjusted to 9.0 by addition of solid carbon dioxide, and the mixture was allowed to react under vigorous stirring in an open flask. After 48 h, the product **6** was isolated as described above (98 mg, 91%, calcd. for heptahydrate). Analytical data were consistent with those given above.

Oxidation of $6^I,6^{IV}$-Dideoxy-$6^I,6^{IV}$-disulfanil-α-cyclodextrin 5 at Variable Concentrations: General Procedure. Compound **5** (10 mg, 9.45×10^{-6} M, calcd for trihydrate) was dissolved in 50 mM aqueous solution of ammonium acetate (1.89 mL, 9.45 and 94.5 mL, respectively; pH 9.0) to prepare three samples with concentrations of 5×10^{-3}, 10^{-3}, and 10^{-4} M. Solutions were stirred vigorously in open flasks at room temperature, and the pH was occasionally checked using pH-meter and, if necessary, adjusted to 9.0 by additions of concentrated aqueous ammonia. After 48 h, the samples were freeze-dried, and the residues were further dried in vacuum for at least 8 h until no traces of ammonium acetate were detected. Samples were analyzed by ^{1}H NMR spectra immediately after dilution in deuteriumoxide.

Equilibration of 6: General Procedure. Compound **6** (5.0 mg, 2.35×10^{-6} mol, calcd for heptahydrate) was dissolved in oxygen-free 50 mM ammonium acetate buffer at pH 9 (0.9 mL) under argon atmosphere. To this solution was added a 1 mM solution of **5** in the same buffer (0.118 mL; 1.18×10^{-7} mol). The solution was then diluted with buffer to obtain five samples with concentrations distributed between 0.1 and 4.7 mM (with respect to the monomer) and allowed to react for 48 h under argon atmosphere. Then the flasks were opened, and remaining traces of **5** were allowed to air-oxidize. The solutions were freeze-dried, residual ammonium acetate was removed in vacuum, and the ratios of **6** and **7** in individual samples were then determined by quantitative ^{1}H NMR analysis in D_2O.

Equilibration of **7** was done using the same protocol as described for **6**.

6-Bromo-6-deoxy-α-cyclodextrin 8. In a Schlenk flask under argon atmosphere was dissolved tetrabromomethane (4.72 g, 14.2 mmol) in dry DMF (23 mL) followed by triphenylphosphane (3.73 g, 14.2 mmol). To the stirring solution was added dried α-cyclodextrin (2.12 g, 2.18 mmol), and the resulting mixture was heated at 40 °C for 48 h. After this period, the reaction was quenched with methanol (4 mL) and poured into acetone (400 mL). The resulting precipitate was filtered off and dried in vacuum. Then it was dissolved in warm water and charged onto reversed-phase column (gradient elution from methanol−water 5:95 to 3:7). Product was isolated as a colorless powder (0.6926 g, 31%): $[\alpha]^{25}_D = +132$ ($c = 0.3$ in H_2O); ^{1}H NMR, see Table S1 (Supporting Information); ^{13}C NMR, see Table S2 (Supporting Information); HR MS (ESI) calcd for $C_{36}H_{59}O_{29}Br$ [M + Na]$^+$ *m*/*z* 1057.2205, found 1057.2223. Anal. Calcd for $C_{36}H_{59}O_{29}Br\cdot 7H_2O$: C, 40.34; H, 5.92. Found: C, 40.43; H, 6.26.

6-Deoxy-6-(thioacetyl)-α-cyclodextrin 9. Compound **8** (303.4 mg, 0.283 mmol, calcd for dihydrate) was dissolved in dry DMF (5.5 mL) in a Schlenk flask equipped with a magnetic stirring bar under argon atmosphere. The mixture was degassed by application of vacuum−argon cycle, and a solution of potassium thioacetate (37 mg, 0.324 mmol) in dry degassed DMF (1 mL) was added dropwise at room temperature. The mixture was allowed to react for 12 h. It was then poured into acetone (60 mL), and the crude product was separated on a sintered glass as a white precipitate.

Subsequent purification by column chromatography (C-18 reversed-phase, column 20 × 170 mm, gradient elution from methanol−water 5:95 to 3:7) afforded white material (275 mg, 89%, calcd for trihydrate): $[\alpha]^{25}_{D} = +152$ ($c = 0.1$ in H_2O); ^{1}H NMR, see Table S1 (Supporting Information); ^{13}C NMR, see Table S2 (Supporting Information); MS (ESI) calcd for $C_{38}H_{62}O_{30}S$ $[M + Na]^+$ m/z 1053.3, found 1053.3. Anal. Calcd for $C_{38}H_{62}O_{30}S \cdot 3H_2O$: C, 42.07; H, 6.32; S, 2.96. Found: C, 42.32; H, 6.29; S, 2.75.

Dimer 10. Compound **9** (240 mg, 0.221 mmol, calcd for trihydrate) was dissolved in water (10 mL), and the solution was deoxygenated by means of triple vacuum−argon cycle. Then a deoxygenated aqueous 1 M solution of sodium hydroxide (1 mL, 1 mmol) was added, and the mixture was allowed to react for 6 h under argon atmosphere. The flask was opened, and methanol (2 mL) was added to the mixture. The pH of the solution was adjusted to 9.0 by addition of solid carbon dioxide, and the mixture was allowed to react under vigorous stirring in an open flask. After 48 h, the solution was neutralized by addition of HCl and charged onto the chromatography column (C-18 reversed-phase, column 16 × 130 mm, gradient elution from methanol−water 5: 95 to 3: 7). The product **10** (194 mg, 80%, calcd. for dodecahydrate) was isolated as a colorless solid material: $[\alpha]^{25}_{D} = +194$ ($c = 0.1$ in H_2O); ^{1}H NMR, see Table S1 (Supporting Information); ^{13}C NMR, see Table S2 (Supporting Information); MS (ESI) calcd for $C_{72}H_{118}O_{58}S_2$ $[M + H]^+$ m/z 1974.6, found 1974.6. Anal. Calcd for $C_{72}H_{118}O_{58}S_2 \cdot 12H_2O$: C, 39.13; H, 6.57; S, 2.90. Found: C, 39.17; H, 6.69; S, 2.79.

Acknowledgment. We thank Joel Tellinghuisen (Vanderbilt University, Nashville, TN) for his helpful comments regarding the analysis of ITC results. Financial support from the Institute (Z40550506) and from grant agencies (GA AVČR, IAA400550810; GA ČR, 203/06/1550 and 203/06/1727; MŠMT OC172 and LC512) is greatly acknowledged.

Supporting Information Available: General experimental methods, Tables of ^{1}H and ^{13}C NMR chemical shifts, copies of ^{1}H and ^{13}C NMR spectra, details for the determination of association constants of inclusion complexes by ITC including copies of selected thermograms, X-ray experimental data, and details of computational procedures. This material is available free of charge via the Internet at http://pubs.acs.org.

JO802139S